Development 139, 709-719 (2012) doi:10.1242/dev.073197

Bmp signaling regulates a dose-dependent transcriptional program to control facial skeletal development

Margarita Bonilla-Claudio[1,2], Jun Wang[1], Yan Bai[1,3], Elzbieta Klysik[1], Jennifer Selever[3,*] and James F. Martin[1,2,3,4,5,‡]

SUMMARY

We performed an in depth analysis of *Bmp4*, a critical regulator of development, disease, and evolution, in cranial neural crest (CNC). Conditional *Bmp4* overexpression, using a tetracycline-regulated *Bmp4* gain-of-function allele, resulted in facial skeletal changes that were most dramatic after an E10.5 *Bmp4* induction. Expression profiling uncovered a signature of Bmp4-induced genes (BIG) composed predominantly of transcriptional regulators that control self-renewal, osteoblast differentiation and negative Bmp autoregulation. The complimentary experiment, CNC inactivation of *Bmp2*, *Bmp4* and *Bmp7*, resulted in complete or partial loss of multiple CNC-derived skeletal elements, revealing a crucial requirement for Bmp signaling in membranous bone and cartilage development. Importantly, the BIG signature was reduced in Bmp loss-of-function mutants, indicating Bmp-regulated target genes are modulated by Bmp dose. Chromatin immunoprecipitation (ChIP) revealed a subset of the BIG signature, including *Satb2, Smad6*, *Hand1, Gadd45γ* and *Gata3*, that was bound by Smad1/5 in the developing mandible, revealing direct Smad-mediated regulation. These data support the hypothesis that Bmp signaling regulates craniofacial skeletal development by balancing self-renewal and differentiation pathways in CNC progenitors.

KEY WORDS: Bone morphogenetic protein, Morphogenesis, Neural crest, Mouse

INTRODUCTION

The CNC is a migratory cell population that originates in the dorsal neural tube and diversifies into multiple cells types, including cartilage, bone, neurons and glia. Much of the craniofacial skeleton such as the skull vault or calvarium, mandible and midface develops through direct, intramembranous ossification of CNC-derived progenitor cells (Chai and Maxson, 2006). For example, in the skull, osteogenesis occurs in discrete areas within the cranial mesenchyme, resulting in the flat bones of the skull forming between the central nervous system (CNS) and overlying ectoderm. The mandible and most midfacial bones develop by direct ossification of CNC-derived branchial arch mesenchyme.

Bmp signaling plays crucial roles in normal craniofacial development, and *Bmp4* deficiency results in craniofacial anomalies, such as cleft lip and palate, in mouse and humans (Liu et al., 2005b; Suzuki et al., 2009). In the mandible, *Bmp4* regulates proximodistal patterning and timing of bone differentiation in mandibular mesenchyme (Liu et al., 2005a; Merrill et al., 2008). There is strong evidence that Bmp signaling regulates craniofacial morphological change during evolution. Both gain-of-function studies and comparative expression data revealed *Bmp4* to be a crucial regulator of beak shape in Darwin's finches, a classic model of evolutionary diversification (Abzhanov et al., 2004; Wu et al., 2004). Other experiments in Cichlid fish also support the notion that *Bmp4* is a major regulator of craniofacial cartilage shape and morphological adaptive radiation (Albertson et al., 2005). However, the downstream genes that Bmp regulates to control facial morphogenesis are poorly understood.

Recent molecular insights into Bmp signaling indicate that the downstream effector mechanisms for Bmp signaling are complex and require further study (Wang et al., 2011). The canonical Bmp pathway involves nucleo-cytoplasmic shuttling of Smad effectors in response to Bmp signaling. In addition, Smad-independent mechanisms that are mediated through MapK pathways are also known to play an important role in tooth development (Xu et al., 2008). More recent work, uncovering a third Bmp effector mechanism, revealed that Smad1/5 directly binds to the Drosha complex to promote microRNA (miR) processing (Davis et al., 2008). In addition, Bmp signaling can induce miR transcription through a canonical Smad-regulated mechanism (Wang et al., 2010). Despite the central importance of Bmp signaling for craniofacial development, congenital defects, and evolution, the mechanisms underlying Bmp action in CNC remains poorly understood.

Here, we have investigated Bmp signaling in CNC development using both gain- and loss-of-function approaches. Inactivation of *Bmp2*, *Bmp4* and *Bmp7* in CNC indicate that *Bmp2* and *Bmp4* are the major Bmp ligands required for development of CNC-derived bone and cartilage. Moreover, gain-of-function studies indicate that elevated *Bmp4* in CNC results in dramatic changes in the facial skeleton. Expression profiling and quantitative RT-PCR (qRT-PCR) studies uncovered a common set of Bmp regulated target genes in both gain- and loss-of-function embryos. A subset of Bmp-regulated targets were directly bound by Smad 1/5, indicating direct regulation. Bmp-regulated genes control self-renewal, osteoblast differentiation and negative feedback regulation, suggesting that Bmp signaling regulates facial skeletal morphogenesis by controlling the balance between self-renewing progenitors and differentiating lineage-restricted cells.

[1]Department of Molecular Physiology and Biophysics, Baylor College of Medicine, One Baylor Plaza, Houston, TX 77030, USA. [2]Program in Genes and Development, University of Texas Graduate School of Biomedical Sciences, Houston, TX 77030, USA. [3]Institute of Biosciences and Technology, Texas A&M Health Science Center, Houston, TX 77030, USA. [4]Program in Developmental Biology, Baylor College of Medicine, One Baylor Plaza, Houston, TX 77030, USA. [5]Texas Heart Institute, Houston, TX 77030, USA.

*Present address: Department of Molecular and Human Genetics, Baylor College of Medicine, 1 Baylor Plaza, Houston, TX 77030, USA
‡Author for correspondence (jfmartin@bcm.edu)

Accepted 28 November 2011

MATERIALS AND METHODS

Mouse alleles and transgenic lines

The generation and characterization of *Bmp2* and *Bmp4* conditional null mice and *Wnt1Cre* transgene mice has been previously described (Chai et al., 2000; Danielian et al., 1998; Liu et al., 2004; Ma and Martin, 2005). The conditional *Bmp7*-null allele will be described elsewhere (Y.B. and J.F.M., unpublished).

Skeletal analysis

Embryos were placed overnight in water and scalded in hot water for 30 seconds. The skin and internal organs were removed and the sample fixed overnight in 95% ethanol. The cartilage was stained with 0.15 mg/ml Alcian Blue (Sigma) in a 1:4 mixture of glacial acetic acid and 95% ethanol. After staining overnight, the samples were rinsed twice in 95% ethanol and incubated for 24 hours in 95% ethanol. In preparation for bone staining, the sample was placed in 2% KOH for 1 hour. Bones were stained using 0.05 mg/ml of Alizarin Red (Sigma) diluted in 2% KOH for 2-4 hours and then cleared with glycerol. For adult skulls, partially dissected heads were placed with Dermestid Beetles (Carolina) to remove soft tissues. After soft tissue removal, skulls were placed in 100% ethanol to remove any remaining beetles, air dried and stored at room temperature.

Alkaline phosphatase staining

E14.5 embryos were dissected, decapitated and fixed in 4% paraformaldehyde for 1 hour. Heads were bisected midsagittally and the brain and dura mater removed, washed three times in PBS and NTMT. The NBT/BCIP (Roche) substrate in NTMT was added until bone staining was observed. Samples were then washed in PBS, and post-fixed in 4% paraformaldehyde.

Western blot

Cell lysates were prepared by dissecting E11.5 mandibles in PBS. Tissue was homogenized in lysis buffer (50 mmol/l Tris, 150 mmol/l NaCl, 1% Triton, 0.5% deoxycholate plus protease inhibitors cocktail; Roche, EDTA and sodium vanadate; Sigma). Protein concentration was determined by the Protein Assay Reagent kit (Pierce). Whole-cell lysates were separated by 12% SDS-PAGE and transferred to nitrocellulose. After blocking with 5% nonfat milk at room temperature for 1 hour, blots were incubated with the p-Smad 1/5/8 polyclonal antibody (1:1000 dilution; Cell Signaling, #9511) and Smad 1/5/8 polyclonal antibody (1:1000 dilution; Santa Cruz, sc-6031 X) at room temperature with agitation for 1 hour, followed by incubation with anti-rabbit IgG horseradish peroxidase-conjugated antibody (1:2000; GE Healthcare). Blots were developed using an enhanced chemiluminescence detection kit (ECL; Pierce). To confirm equal loading, we used anti-β-actin antibody (1:5000; Sigma). Western blots were quantified by densitometry analysis using Image J software (NIH).

Histology and whole-mount in situ hybridization

Hematoxylin-Eosin staining and whole-mount in situ hybridization were performed as previously described (Wang et al., 2010). Plasmids for in situ probes have been previously described: *Dlx6* (Charite et al., 2001), *Gata3* (Ruest et al., 2004), *Hand1* (McFadden et al., 2005), *Smad6* (Ma et al., 2005), *Msx1* (Ishii et al., 2005), *Msx2* (Ishii et al., 2003) and *Tbx20* (Shen et al., 2011). Full-length cDNA for mouse BMP4 was provided by Dr Stephen Harris (UTHSC, San Antonio, TX, USA) and was linearized with *Spe*I and transcribe with T7. Exons 3 and 4, including 3′UTR of *Gadd45g* were amplified and subcloned into T-easy vector. Plasmid was linearized with *Eco*RV and transcribed with T7 RNA polymerase. Cux2 (exon 23) and Satb2 (exon 10) were amplified and subcloned into T-easy vector. Plasmid was linearized with *Sac*I and transcribed with T7 RNA polymerase. For all experiments, at least three mutants and three controls embryos were analyzed for each probe.

Generation of the Bmp4 Tet operator allele

To generate the $Bmp4^{tetO}$ allele, we constructed a targeting vector that resulted in a 665 bp deletion upstream of and including the *Bmp4* basal promoter and *Bmp4* exon 1. We modified the tetO plasmid, a kind gift from Raymond MacDonald's laboratory (UT Southwestern Medical Center, TX, USA), which contains the tetracycline operator (tetO7), CMV promoter, IRES-*lacZ* and a poly-adenylation sequence. *Bmp4* genomic DNA was isolated from the 129/S BAC library. A 9 kb *Eco*RI fragment of *Bmp4* genomic DNA was subcloned into pBluescript (Stratagene). We inserted *Bmp4* cDNA into *Not*I and *Kas*I sites downstream of the tetO7 and CMV promoter. The *phosphoglycerol kinase neomycin*-resistance cassette (*pgk-neo*) with two flanking Frt sites was blunt cloned into the *Asc*I site downstream of the IRES-*lacZ*. The 3 kb 3′ homology arm was amplified by PCR using the primers (5′ to 3′) tgagcagggcaacctggagaggg and tccgaatggcactacggaatggct, and blunt-end ligated into a *Swa*I site downstream of *pgk-neo*. The $Bmp4^{tetO}$ 5′ arm, 1.7 kb *Eco*RI-*Apa*LI fragment, was cut from *Bmp4* genomic DNA and blunt end cloned into *Xho*I site upstream of the tetO7. The targeting construct was linearized with *Pme*I and electroporated into AK7 embryonic stem cells, selected in G418, and screened by Southern blot. The cells were digested with *Eco*RV and *Bmp4* exon 4 was used as the 3′ flanking probe. Wild-type allele gives a 22 kb *Eco*RV fragment and the targeted allele gives a 16 kb *Eco*RV fragment. The targeting frequency for the tetO allele is 4.2% (7/167). We also used a *Spe*I digest to confirm correct targeting: the wild-type band was 6.4 kb, the cDNA band was 11.7 kb and the mutant allele was 8.0 kb. We used the Rosa 26 rtTA allele (Belteki et al., 2005) to express the reverse tetracycline activator (Tet-on) under the control of the *Wnt1*Cre allele. This will drive $Bmp4^{tetO}$ allele expression in neural crest cells in the presence of doxycycline.

Doxycycline administration in mice

Pregnant females were given doxycycline (Sigma) in the drinking water (2 mg/ml) and in the food (Bio-Serv; 200 mg/kg), for a 24 hour period unless otherwise specified.

Quantitative real-time PCR and microarray

E11.5 mandibles were dissected in ice-cold PBS and placed in RNAlater (Ambion) for RNA stabilization. mRNA was then extracted using the RNeasy Micro Kit (Qiagen). First strand cDNA synthesis was then performed utilizing the SuperScript II Reverse Transcriptase kit (Invitrogen) with 500 ng of mRNA. Quantitative real-time PCR was performed using SYBR Green QPCR Master Mix (Invitrogen) in triplicate reactions and ran on Mx3000P thermal cycler (Stratagene). Primers used in this study are listed in supplementary material Table S2. For all qRT-PCR experiments, at least three mutants and three controls embryos were analyzed. DNA microarray analysis, including gene ontology analysis, was performed using the OneArray Mouse Whole Genome Array (Phalanx Biotech Group). Mandibular processes were pooled to collect a minimally required RNA amount: seven *Bmp4* OE and five controls embryos were used. Gene ontology results were confirmed using DAVID Bioinformatics Resources 6.7 National Institute of Allergy and Infectious Diseases (NIAID), NIH. Microarray data have been submitted to Gene Expression Omnibus (Accession Number GSE35402).

Chromatin immunoprecipitation

Chromatin immunoprecipitation (ChIP) analysis was performed as previously described (Wang et al., 2010). We used E11.5 wild-type mice mandibles and the mouse osteoblastic cell line *MC3T3*-E1 (ATCC). Cells where maintained and propagated following ATCC protocols. Experiments were performed with 90% confluent cultures and Bmp4 (R&D System) was added to the media for a final concentration of 25 pg/μl for 12 hours. Primer sequences used for amplification of the Bmp/Smad regulatory elements are found in supplementary material Table S2.

Sequence analysis

For sequence analysis and multiple sequence alignment, Ensembl genome database and MAFFT (http://mafft.cbrc.jp/alignment/server/) were used.

RESULTS

Bmp2, *Bmp4* and *Bmp7* deletion in cranial neural crest results in severe loss of cranial bone

We used the *Wnt1Cre* driver and a *Bmp4* conditional null allele, $Bmp4^{floxneo}$, to inactivate *Bmp4* in CNC (Chai et al., 2000; Liu et al., 2004). Intercrosses between *Wnt1Cre*; $Bmp4^{floxneo/+}$

with *Bmp4*^{floxneo} homozygous mice generated *Wnt1Cre*; *Bmp4*$^{floxneo;floxneo\ (f/f)}$ mutant embryos, hereafter called *Bmp4* CKO. Evaluation of skull preparations indicated that *Bmp4* CKO mutant newborn skulls had enlarged frontal fontanelle and subtle mandibular defects (Fig. 1A,B). Examination of *Msx1* and *Msx2* expression, markers of preosteogenic head mesenchyme, revealed that these markers were reduced but still present in the *Bmp4* CKO embryos (supplementary material Fig. S1A-D). Alkaline phosphatase, a marker of both preosteoblasts and mature osteoblasts, was also reduced in the frontal bone of *Bmp4* CKO embryos, indicating a defect in the transition from pre-osteoblast to osteoblast in the *Bmp4* CKO (supplementary material Fig. S1E,F). Persistent Msx gene expression in *Bmp4* CKO embryos suggested that other Bmp ligands probably had overlapping functions with *Bmp4* in CNC.

To test this idea, we generated compound conditional loss-of-function mutants for *Bmp2*, *Bmp4* and *Bmp7* using Bmp conditional null alleles and the *Wnt1Cre* driver. The genetic analysis indicated that although *Bmp4* was the major functional Bmp ligand in CNC-derived bone development, *Bmp2* also had important functions.

Analysis of *Bmp4* and *Bmp7* compound mutants indicated that *Bmp7* failed to have a significant influence on *Bmp4* CKO mutant phenotype (Fig. 1A-E,R). By contrast, *Bmp2* deletion in the *Bmp4* CKO background resulted in a significant worsening of frontal and mandibular bone phenotypes. The *Bmp2/4* CKO mutant had a drastic reduction in most CNC-derived bones such as the frontal and mandible (Fig. 1F-I,S). Additionally, *Bmp2* had a unique role in coronoid process development (Fig. 1G,K,N). Analysis of triple-mutant combinations further supported the conclusion that *Bmp4*

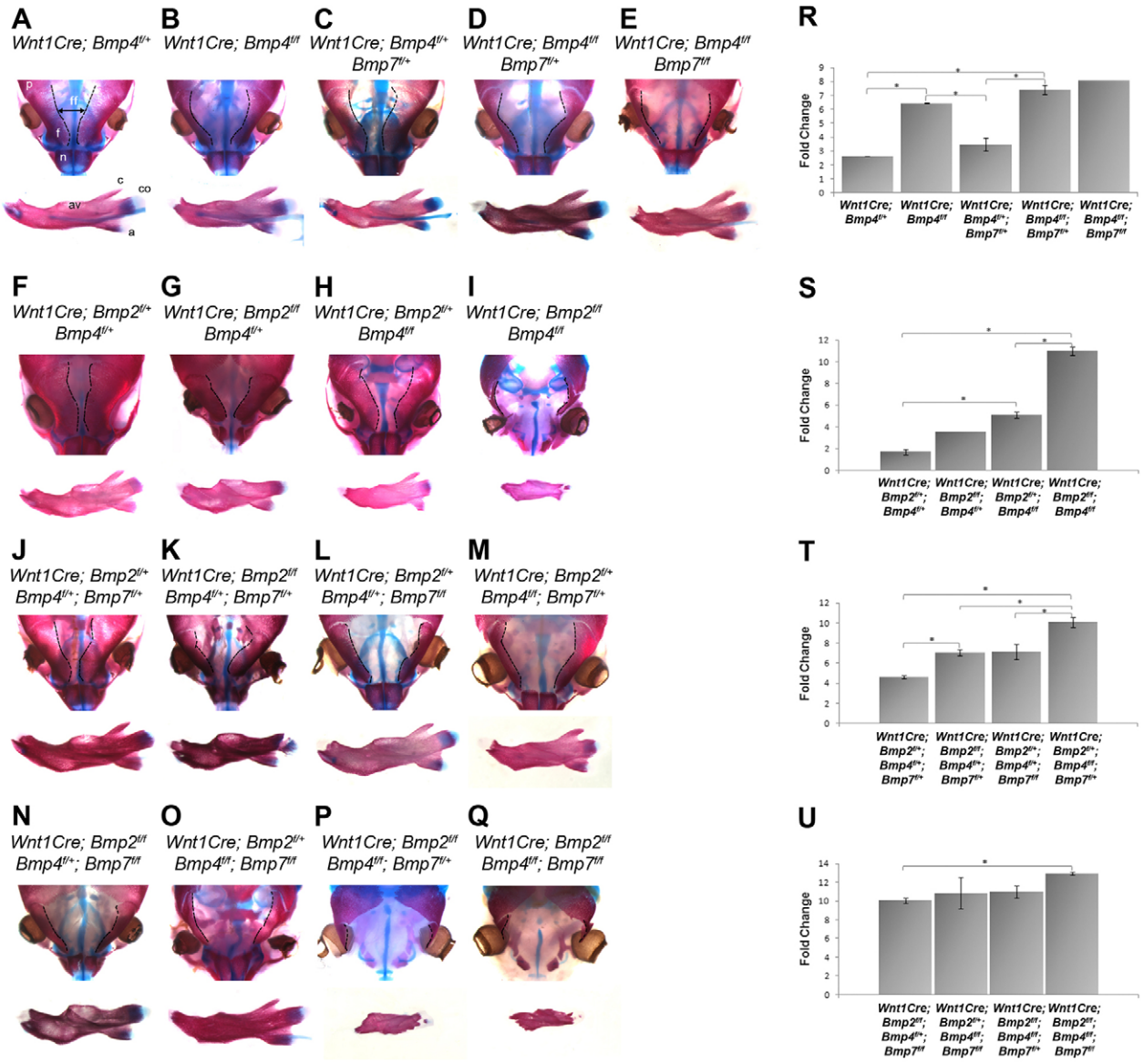

Fig. 1. Increased severity of craniofacial defects in Bmp compounds mutants. (**A-Q**) Alcian Blue/Alizarin Red stains of E18.5 embryo showing defects in the frontal and mandible bone. Arrow in A indicates the distance between the frontal bones use to measure the frontal fontanelle for each genotype. a, angular process; av, alveolar bone; c, coronoid process; co, condylar process; f, frontal bone; ff, frontal fontanelle; n, nasal bone; p, parietal bone. (**R-U**) Increase in the frontal fontanelle size of the Bmp compounds mutants when compared with littermate control. **P*<0.05. Data are mean±s.e.m.

and *Bmp2* were the major ligands in frontal and mandibular bone development. Comparison between embryos that were *Bmp2; Bmp4* compound homozygous and were either $Bmp7^{+/+}$, $Bmp7^{flox/+}$ or $Bmp7^{flox/flox}$ indicated that *Bmp7* has a minor role in frontal bone formation (Fig. 1I,P,Q). In addition to the frontal and mandibular bone defects, other CNC derived bones were affected in Bmp compound mutants (supplementary material Fig. S2).

A tetracycline-regulated *Bmp4* gain of function allele

We next tested the role of elevated Bmp4 signaling in CNC. We developed a tetracycline-regulated *Bmp4* allele ($Bmp4^{tetO}$) by replacing the first non-coding exon and basal promoter region of *Bmp4* with a *tet operator Bmp4* cDNA fusion gene (Fig. 2A,B). We used a cre-recombinase inducible *rtTA* (Tet-on) allele, $R26R^{rtTANagy}$ allele and the *Wnt1Cre* allele to induce rtTA in the CNC lineage (Belteki et al., 2005). *Bmp4* was overexpressed by inducing *Wnt1Cre*; $Bmp4^{tetO/+}$; $R26R^{rtTANagy}$ (*Bmp4* OE) embryos with doxycycline (dox) (Fig. 2C).

To determine whether *Bmp4* OE embryos had elevated *Bmp4* levels in CNC, we dissected mandibular processes from *Bmp4* OE and control embryos and performed qRT-PCR. *Bmp4* OE embryos had approximately 30-fold inducible *Bmp4* upregulation. Furthermore, *Bmp4* levels were increased with higher levels of dox (Fig. 2D). *Bmp4* induction could be detected 3 hours after dox induction and increased through 24 hours of induction (Fig. 2E). Elevated *Bmp4* was also detectable in CNC by whole-mount in situ in E11.5 embryos (Fig. 2F). Western blot indicated that the elevated *Bmp4* mRNA expression resulted in approximately a 2.5-fold increase in p-Smad1/5/8 activity in the mandibular process (Fig. 2G). In addition, p-Smad1/5/8 activity in the $Bmp4^{tetO}$ heterozygous embryos was reduced when compared with the wild-type control, indicating that $Bmp4^{tetO}$ allele is a *Bmp4* hypomorphic allele (Fig. 2G; supplementary material Fig. S3). Analysis of $Bmp4^{tetO}$ homozygous mutant embryos supported the conclusion that $Bmp4^{tetO}$ is hypomorphic (supplementary material Fig. S3).

Facial development is dramatically altered by elevated Bmp4 in CNC

We evaluated the phenotypic effect of elevated *Bmp4* expression in CNC by analyzing E16.5 *Bmp4* OE embryos that had been induced at embryonic stages between E10.5 and E14.5. *Bmp4* induction at E13.5 resulted in a mandible that was more pointed in appearance although overall facial form was not significantly changed (Fig. 3A-D). *Bmp4* induction at E11.5 resulted in a mandible that was shorter and more pointed than the control (Fig. 3E-H). In E10.5 *Bmp4*-induced embryos, the face was drastically changed. There was shortening and pointed appearance in both the mandible and maxilla. The overall shape of the head was more rounded when compared with the control mouse embryo. Moreover, the orientation of the eyes was more anterior when compared with the control (Fig. 3I-L).

Skeletal preparations indicated that, at E10.5, *Bmp4* induction resulted in strong reduction of rostral bony elements, such as nasal bones, with a drastically shortened face (supplementary material Fig. S4G,H). Overall bone quality was defective in that skull bones revealed multiple translucent areas. *Bmp4* induction at E12.5 had less dramatic morphological changes but the size of the nasal cartilages was expanded while nasal and frontal bones were absent or reduced (supplementary material Fig. S4E,F) and the mandible was shorter. Induction at E13.5 revealed reduction in nasal bones and coronoid process of the mandible (supplementary material Fig. S4C,D).

Histological analysis indicated that *Bmp4* E12.5 induction resulted in a large increase in both nasal and Meckel's cartilage, indicating that *Bmp4* modulates both cartilage and bone development (supplementary material Fig. S5A-D,I-L). These *Bmp4* E12.5 induced embryos also had cleft palate (supplementary material Fig. S5K). Embryos induced at E14.5 showed milder phenotypes, indicating that *Bmp4*-induced facial changes are stage dependent (supplementary material Fig. S5E-H).

Expression profiling uncovers transcriptional regulators that are upregulated in the mandible of *Bmp4* gain-of-function embryos

To comprehensively investigate genes regulated by Bmp signaling in the mandibular process, we performed expression profiling using RNA extracted from E11.5 *Bmp4* OE mandibles that were induced with dox for 24 hours. Using a twofold change ($P<0.05$) as threshold, we identified 144 downregulated and 120 upregulated genes (supplementary material Fig. S6A and Table S1). Although gene ontology analysis for all genes revealed several gene clusters involved in multiple cellular processes, among *Bmp4*-induced genes, gene ontology indicated that transcriptional regulation was the main cellular process influenced (supplementary material Fig. S6B,C).

Included in the induced BIG signature after qRT-PCR validation were multiple transcription factor families, including Gata genes, Hand genes, Satb genes and Klf genes (Fig. 4A,B). Other upregulated transcriptional regulators include *Atf3*, *Cux2* and *Isl1*. *Gata3*, *Hand1* and *Satb2* are transcription factors that play important roles in craniofacial development (Fig. 4A,B). Importantly, many of these genes (such as *Isl1* and *Id1*) have been shown to be targets of Smad-mediated signaling in other developmental processes and many have known roles in craniofacial development (Chai and Maxson, 2006). Interestingly, negative regulators of Bmp-Smad signaling, *Gadd45* and *Smad6,* and *Noggin*, were also strongly upregulated in the *Bmp4* OE mandibles, uncovering a negative-feedback pathway in the mandible. We validated the microarray results by qRT-PCR using independently generated RNA from control and *Bmp4* OE mandibles (Fig. 4B). We also looked at expression of essential transcriptional regulators of cartilage and bone, *Runx2* and *Sox9*, in *Bmp4* OE mandibles. Interestingly, although *Sox9* was significantly upregulated, *Runx2* was mildly downregulated, suggesting that Bmp may regulate osteoblast genes both cooperatively and independently of *Runx2* (supplementary material Fig. S7).

In situ hybridization demonstrated an expanded expression pattern of the BIG signature after *Bmp4* induction (Fig. 4C; supplementary material Fig. S8). Interestingly, there were distinct upregulated gene expression patterns. Some genes, such as *Hand1* and *Smad6*, were broadly expanded throughout the CNC, whereas other genes, such as *Gadd45g* and *Satb2*, were expanded in a more restricted region of the mandible (Fig. 4C).

Commons target genes that are expanded in the Bmp4 OE embryos are also downregulated in Bmp loss of function embryos

To determine whether the BIG signature was also reduced in the Bmp loss-of-function embryos, we evaluated the expression of the candidate genes in Bmp-deficient embryos. Because the *Wnt1Cre; Bmp2/4/7* triple mutants are recovered at low frequencies, we supplemented our experiments with the *Nkx2.5Cre*; $Bmp4^{n/f}$ embryos that have greatly reduced Bmp signaling in the mandibular ectoderm and mesenchyme (Liu et al., 2005a). qRT-PCR analysis of the mandibular tissue showed significant reduction

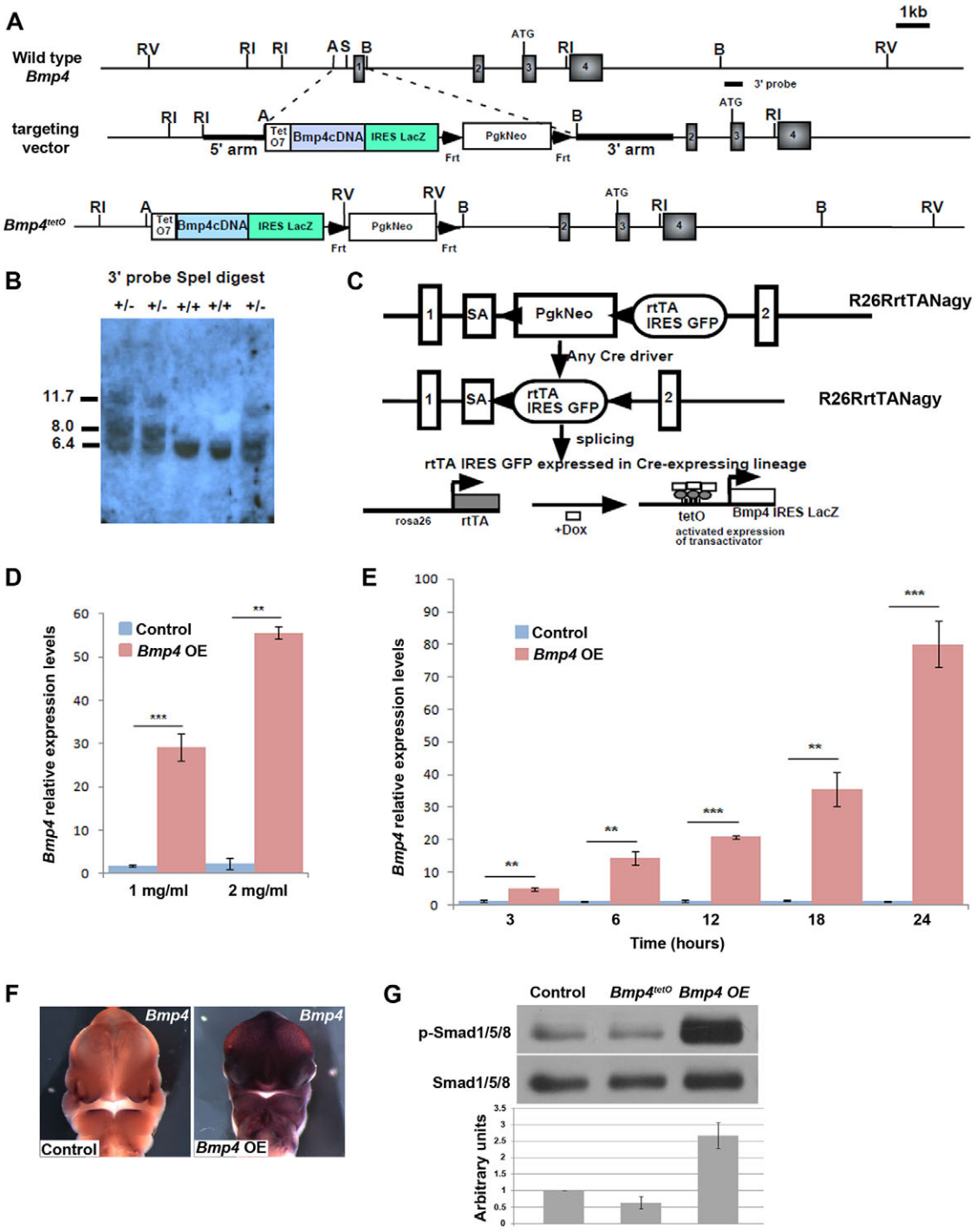

Fig. 2. Overexpression of *Bmp4* using doxycycline-regulated system. (**A**) Targeting vector of *Bmp4*^{tetO} allele, which contains the tetracycline operator (tetO7), CMV basal promoter, *Bmp4* cDNA, IRES-lacZ and *PGK-neo* resistance cassette with two flanking Frt sites, targeted in *Bmp4* basal promoter and *Bmp4* exon1. (**B**) Clones were screened by Southern blot, showing correct targeting by a *Spe*I digestion: the wild-type band was 6.4 kb, the cDNA band was 11.7 kb and the mutant allele was 8.0 kb. (**C**) Schematic illustrating the strategy to regulate spatial and temporal expression of *Bmp4* using the *R26RrtTANagy* allele (Belteki et al., 2005). (**D**) qRT-PCR of E11.5 mandibles showing the response of the *Bmp4*^{tetO} allele to different concentration of doxycycline. (**E**) qRT-PCR of E11.5 mandibles showing the response of the *Bmp4*^{tetO} allele to doxycycline at different periods of time. (**F**) In situ hybridization showing total levels of *Bmp4* transcript after 24 hours of doxycycline (2 mg/ml). (**G**) Western blot and densitometry (n=3) analysis of E11.5 mandibles after 24 hours of doxycycline (2 mg/ml), 10 µg protein/lane. $^{**}P$<0.01, $^{***}P$<0.001. Data are mean±s.e.m.

in the expression levels of genes that were upregulated in the *Bmp4* OE tissue (Fig. 5A). Moreover, whole-mount in situ analysis for a subset of these genes revealed loss of mandibular expression in *Bmp4* mutant embryos (Fig. 5B). qRT-PCR data from *Wnt1Cre; Bmp2/4/7* triple mutant mandibles was consistent with the data from the *Nkx2.5Cre*; *Bmp4*$^{n/f}$ embryos (data not shown).

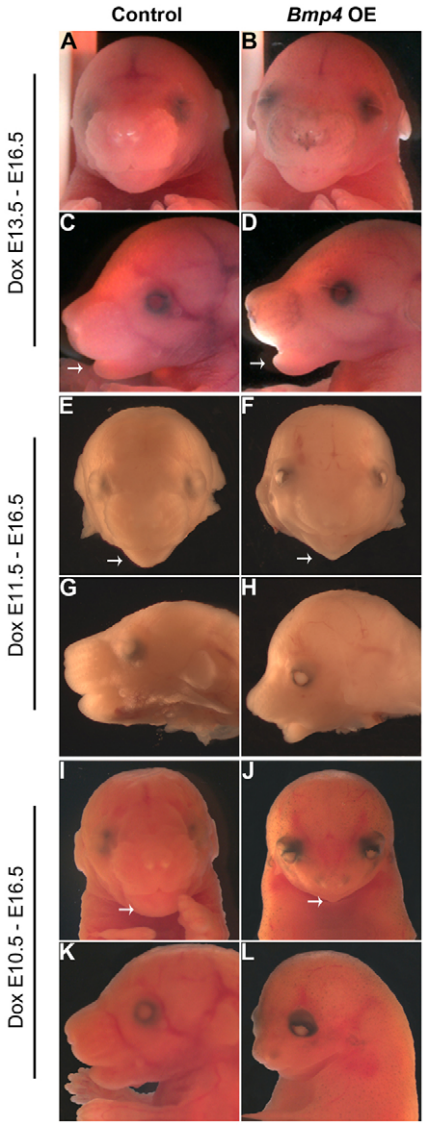

Fig. 3. Morphological changes in the craniofacial region after *Bmp4* overexpression. (**A-L**) Frontal and lateral views of E16.5 control and *Bmp4* OE embryos after induction starting at E13.5 (A-D), E11.5 (E-H) and E10.5 (I-L). Arrows indicate the morphological changes in the mandible.

Subsets of transcriptional regulators are direct *Bmp4* targets

To determine whether genes in the BIG signature were directly regulated by Smad-mediated transcription, we undertook a bioinformatic approach to identify conserved Smad recognition elements within a 5 kb region located in the 5′ flanking region of these genes. For *Gadd45g*, *Gata3*, *Hand1*, *Satb2* and *Smad6*, we uncovered phylogenetically conserved Smad recognition elements (Fig. 6A). We tested the ability of Smad1/5 to bind to these sequences in vivo by ChIP assays in wild-type mandibles and in the mouse osteoblastic cell line *MC3T3*-E1. Our data indicate that in the developing mandible, Smad1/5 binds directly to the chromatin of these five genes (Fig. 6B). Moreover, in MC3T3-E1 cells that were cultured in the presence of Bmp4, we found an enrichment in Smad1/5 chromatin binding after Bmp treatment (Fig. 6C).

DISCUSSION

We performed a comprehensive analysis of Bmp function in CNC using genetics, gene expression profiling and ChIP. Our profiling and qRT-PCR validation data from the *Bmp4* OE embryos indicate that the BIG signature contains 21 genes. Moreover, we validated 17 of the 21 genes in the Bmp loss-of-function model.

Within the BIG signature are transcriptional regulators important for osteoblast differentiation and progenitor cell self-renewal. Bmp signaling also induces a negative regulatory pathway that probably functions as a buffering mechanism to maintain precise Bmp signaling levels. We show that five genes, *Gata3*, *Gadd45*, *Hand1*, *Satb2* and *Smad6*, are directly bound by Smad1/5. Our findings suggest that a balance between self-renewal and progenitor differentiation in CNC underlies Bmp-regulated facial skeletal development (Fig. 6D).

Direct Bmp target genes have been implicated in progenitor cell self-renewal

Our data show that Bmp signaling in CNC progenitors regulates genes that are directly implicated in self-renewal such as Id and Klf genes. *Klf2* and *Klf5*, as well as *Id1* and *Id4* are regulated by Bmp signaling in CNC progenitors. Klf genes, regulators of ES cell self-renewal through the control of *Nanog* expression and cellular reprogramming, have not been shown to be regulated by Bmp signaling. Our findings suggest that Bmp signaling in CNC promotes self-renewal of CNC cells that allow progenitor cells to persist as craniofacial development progresses.

In other in vivo models systems such as the *Drosophila* ovary, Bmp signaling promotes self-renewal and proliferation of somatic stem cells and prolongs progenitor lifespan (Kirilly et al., 2005). In CNC progenitors, it is conceivable that Bmp signaling increases the number of self renewing progenitor cells in addition to activating expression of the CNC self-renewal program.

In addition to inducing *Id1* expression in embryonic stem cells, Bmp signaling directly promotes self-renewal in collaboration with leukemia inhibitory factor through a direct interaction between Smad1 and the core self-renewal factors Nanog, Oct4 and Sox2 (Chen et al., 2008; Fei et al., 2010; Ying et al., 2003). As defined by ChIP seq, Smad1 commonly occupies Nanog-Oct4-Sox2 bound loci, revealing that Bmp signaling directly interacts with the core pluripotency machinery to enhance pluripotency and self-renewal (Chen et al., 2008). Moreover, the Smad1-containing complexes in ES cells recruit the HAT p300 to activate gene transcription. Our findings support a model in which Bmp signaling enhances CNC progenitor self-renewal by activating the self-renewal gene program (Fig. 6D). Future ChIP seq experiments will be required to determine whether Smad1 directly interacts with a pluripotency program in CNC progenitors.

Bmp promotes skeletal differentiation from CNC progenitors

Bmp signaling also regulates lineage-restricted genes such as *Satb2* that enhance osteoblast lineage development. *Satb2* is a DNA-binding and architectural factor that has a positive role in osteoblast development. *Satb2* deficiency results in phenotypes that are similar to mild Bmp loss-of-function phenotypes such as cleft palate and calvarial defects with shortened mandible. Importantly, *Satb2* controls osteoblast differentiation through regulation of *Runx2* and *Atf4* expression (Dobreva et al., 2006). Notably, similar to *Bmp4*, *Satb2* deficiency causes orofacial clefting in humans as well as mice (Britanova et al., 2006). Our data showing that *Satb2*

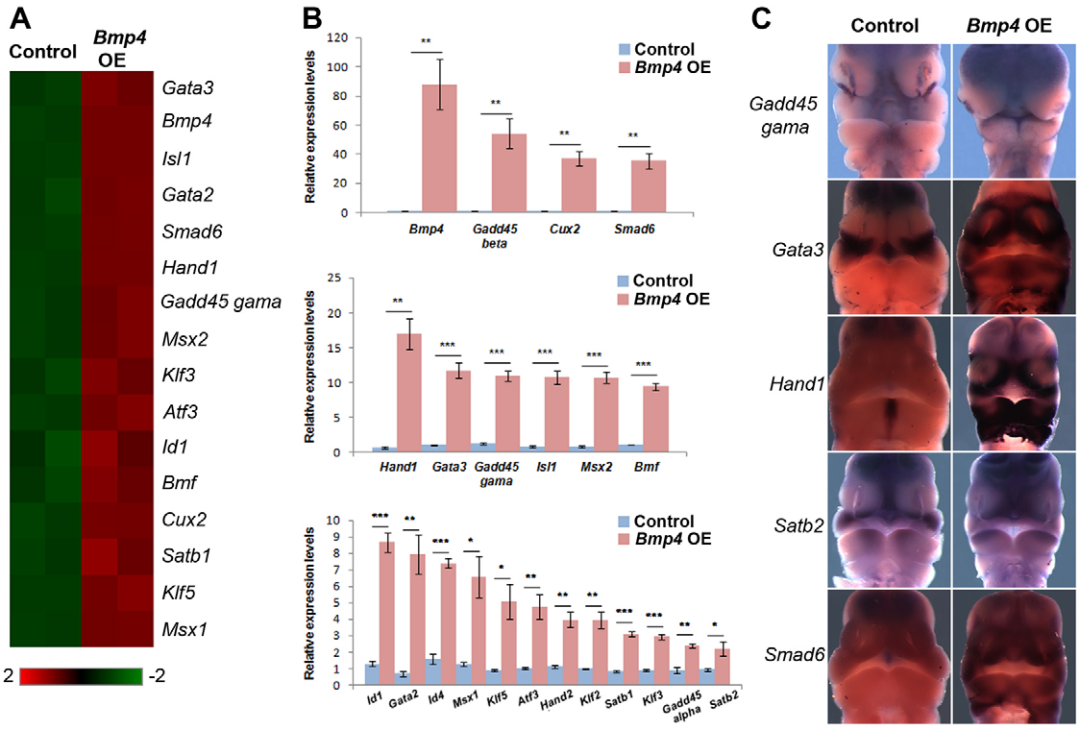

Fig. 4. *Bmp4* gain of function in neural crest cells leads to upregulation of different transcriptional regulators. (**A**) Heat map representing 16 transcriptional regulators that were upregulated in *Bmp4* OE mandibles. (**B**) qRT-PCR validation of microarray results. Other genes from the same family were also included. (**C**) In situ hybridization on E11.5 embryos showing the change in the expression pattern of the indicated genes in the *Bmp4* OE. **P*<0.05, ***P*<0.01, ****P*<0.001. Data are mean±s.e.m.

is a direct Smad1/5 target indicate that a major pathway for Bmp-regulated facial bone development is through *Satb2* function (Fig. 6D).

Similar to *Bmp4* loss-of-function mutants, *Gata3* mutants have a medial mandibular deficiency (Liu et al., 2005a; Ruest et al., 2004). There is evidence that *Gata3* directly regulates *Nmyc* in the branchial arches, suggesting that one cellular mechanism in the *Gata3* mutant mandible is reduced proliferation. Other data also indicate that *Gata3* promotes osteoblast and neuron survival, suggesting that, in addition to proliferation, apoptosis may also be enhanced in *Gata3* mutants as it is in *Bmp4* loss-of-function embryos (Chen et al., 2010; Liu et al., 2005a; Tsarovina et al., 2010).

Hand1 and *Hand2* have overlapping function in medial mandible development, and promote progenitor cell proliferation and inhibit differentiation (Barbosa et al., 2007; Funato et al., 2009). In the heart, *Hand1* overexpression increases cell proliferation, indicating that the Hand mandibular defect may result from reduced progenitor cell proliferation. It is interesting to note that both *Hand1* and *Gata3* have been implicated in trophoblast development, indicating that these two genes may have interrelated functions in multiple cellular contexts (Ralston et al., 2010).

In addition to Bmp signaling, the endothelin (Edn) signaling pathway regulates *Hand* gene expression and also is crucially important in facial form regulation. In zebrafish, an interplay between Bmp and Edn signaling is important for branchial arch dorsoventral patterning (Alexander et al., 2011; Zuniga et al., 2011). *Edn*-deficient embryos display mandibular-to-maxillary transformations that are restricted to the Hox-negative CNC (Gitton et al., 2010). Moreover, gain-of-function experiments indicate that expanded *Edn* and *Hand2* in maxillary process results in transformation to a mandibular phenotype. Our data indicate that Bmp and Edn signaling converge on Hand gene function to regulate facial development.

The *Dlx5/6* genes, targets for Edn signaling and direct regulators of *Hand2*, are also crucially important in facial development (Depew et al., 2002). Only modest *Dlx6* expansion in *Bmp4* OE embryos indicates that Bmp induced regulation of Hand genes primarily goes directly through Smad1/5 (supplementary material Fig. S8).

Bmp-regulated negative-feedback loops are critical for mandible development

Negative autoregulation is a mechanism to confer robustness to the developing embryo by buffering the system from elevated Bmp levels and is crucial for normal craniofacial and heart development (Paulsen et al., 2011; Prall et al., 2007). The negative regulatory loop also probably has an impact on the severity of craniofacial phenotypes that we observed. For example, in *Wnt1Cre; Bmp7* CKO embryos, our preliminary data indicate that *Bmp2*, but not *Bmp4*, expression is upregulated, suggesting that *Bmp7* inhibits *Bmp2* expression through an unknown mechanism. This autoregulation may account for the relatively mild phenotypes seen in *Bmp7* mutant embryos.

Bmp4-induced expression of negative regulators of Bmp signaling such as *Smad6*, *Noggin* and *Gadd45g* (Fig. 6D). The importance of finely tuned Bmp signaling levels in mice and humans is apparent from *Noggin* loss-of-function studies in mice, as well as human genetics studies. *Noggin* deficiency

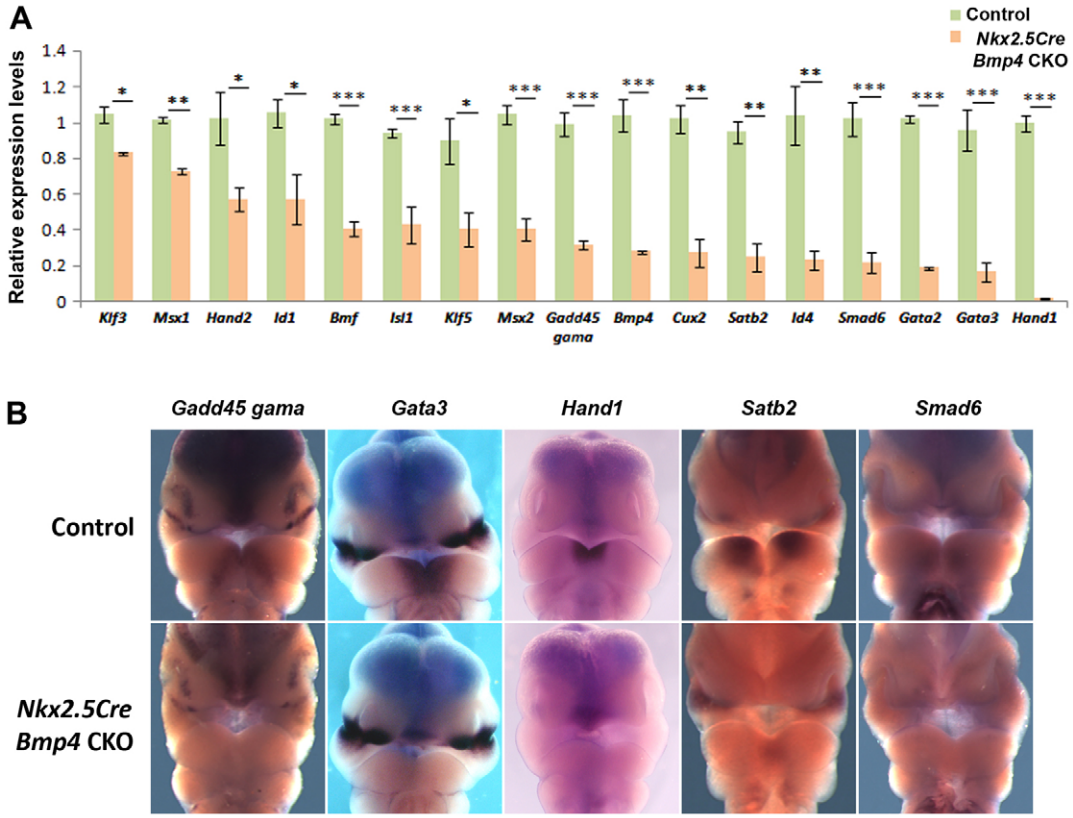

Fig. 5. Bmp deficiency results in reduced expression of Bmp-regulated genes. (**A**) qRT-PCR of E11.5 control and *Nkx2.5Cre;Bmp4* CKO mandibles. **P*<0.05, ***P*<0.01, ****P*<0.001. Data are mean±s.e.m. (**B**) In situ hybridization on E11.5 embryos showing the change in the expression pattern of the indicated genes in the *Nkx2.5Cre;Bmp4* CKO.

results in cleft palate, defective mandibular development, as well as limb and heart defects (Brunet et al., 1998; Choi et al., 2007; Gong et al., 1999; He et al., 2010). The negative auto-regulatory pathway includes two genes, *Gadd45g* and *Smad6*, that are Smad-regulated direct Bmp targets. Moreover, the induced negative regulatory genes modulate the pathway by multiple mechanisms. *Smad6* inhibits R-Smad activity by both competing for Smad4 and also inhibiting R-Smad phosphorylation. *Gadd45g* promotes ubiquitin ligase interaction with the Smad linker region to destabilize R-Smad, while Noggin is a competitive inhibitor of the Bmp ligand-receptor interaction (Sheng et al., 2010).

Bmp signaling controls expression of multiple families of transcriptional regulators

Cux2 has not been previously connected to Bmp signaling or bone morphogenesis. The closely related gene *Cux1* is regulated by Tgfβ and represses collagen expression (Fragiadaki et al., 2011). *Cux2* is regulated by Notch signaling in the spinal cord, where it controls the balance between neural progenitors and differentiated neurons by modulating cell cycle progression and enhancing interneuron fate (Iulianella et al., 2008; Iulianella et al., 2009). Interestingly, Notch has been shown to work in parallel with Bmp signaling in valve development, suggesting that Notch and Bmp signaling may work together to regulate the balance of CNC progenitors with differentiated skeletal cells (Luna-Zurita et al., 2010).

The BIG signature contains genes that are known to be Bmp regulated. Previous experiments uncovered a Bmp-Msx genetic pathway in multiple contexts within the developing craniofacial apparatus, including skull, palate and teeth (Chai and Maxson, 2006). Our data also indicate that *Isl1*is regulated by Bmp signaling during mandibular development. There is evidence that Bmp and *Isl1* function in a positive-feedback loop in the mandible (Mitsiadis et al., 2003). Our data support these earlier findings and substantially extend previous understanding of Bmp targets in craniofacial development.

Bmp target spatial regulation in contrast to quantitative regulation

Our in situ data indicate that in the *Bmp4* OE embryos one gene group, including *Gata3*, *Hand1* and *Smad6* was broadly expressed throughout the cranial neural crest in response to *Bmp4* overexpression. By contrast, genes such as *Satb2* and *Gadd45g* were more resistant to *Bmp4* overexpression and were upregulated in a more discrete spatial pattern. This observation indicates that other regulatory mechanisms, such as microRNA (miR)-mediated regulation, fine-tune the expression of *Satb2* and *Gadd45g*. miRs are small non-coding RNAs that post transcriptionally regulate gene expression by enhancing mRNA degradation or by inhibiting translation (Bartel, 2009). One idea is that other signaling pathways, such as Notch or Wnt, may regulate miR expression that then degrades target mRNAs in specific domains of the branchial arches. Alternatively, the distinct responses to Bmp4 signaling may

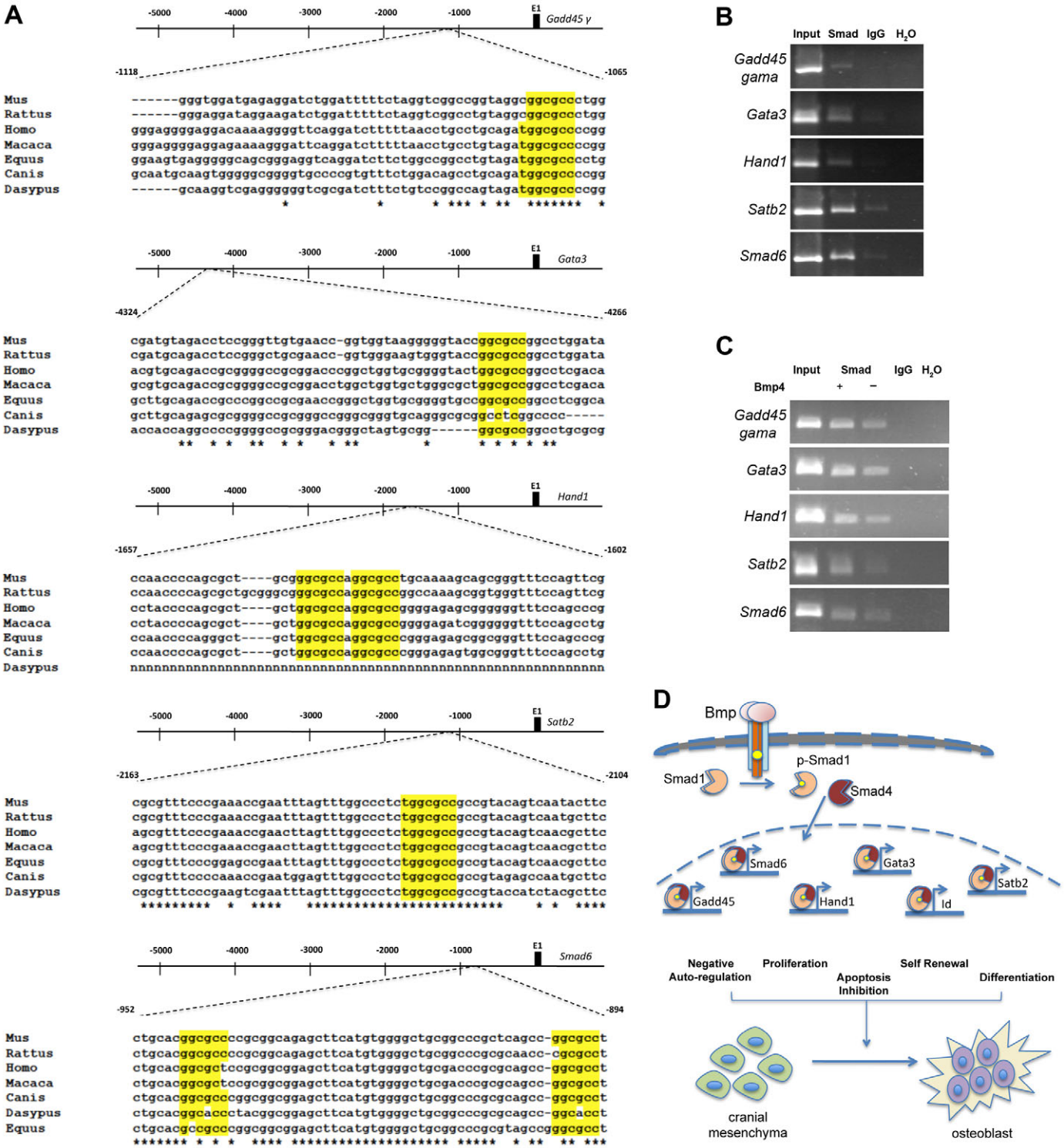

Fig. 6. Direct Smad-mediated regulation of a subset of Bmp-induced genes. (**A**) Sequence alignment showing the conservation among species of the putative Smad- binding site. (**B**,**C**) ChIP assay using (B) E11.5 wild-type mandibles and (C) MC3T3-E1 cells culture for 12 hours in the absence or presence of 25 pg/µl of Bmp4. (**D**) Proposed model where Bmp regulates craniofacial skeletal development by direct regulation of genes involved in self-renewal, proliferation, apoptosis and differentiation of the CNC progenitors.

be regulated at the level of chromatin regulation such that Smad-mediated activation is offset by negative regulatory mechanisms that cannot be overcome by high levels of Bmp signaling. Future experiments are required to investigate these ideas.

Acknowledgements
We thank A. Bradley, and R. Johnson for reagents, and James Douglas Engel, Richard Maas, Robert E. Maxson, Jr, Sylvia Evans and Stephen E. Harris for in situ probes. Part of this work was included within the PhD theses of J.S. and M.B.-C.

Funding
Supported by the National Institutes of Health (NIH) [2R01DE/HD12324-14 to J.F.M. and 5T32DE015355 to M.B.-C.]. Deposited in PMC for release after 12 months.

Competing interests statement
The authors declare no competing financial interests.

Supplementary material
Supplementary material available online at
http://dev.biologists.org/lookup/suppl/doi:10.1242/dev.073197/-/DC1

References
Abzhanov, A., Protas, M., Grant, B. R., Grant, P. R. and Tabin, C. J. (2004). Bmp4 and morphological variation of beaks in Darwin's finches. *Science* **305**, 1462-1465.
Albertson, R. C., Streelman, J. T., Kocher, T. D. and Yelick, P. C. (2005). Integration and evolution of the cichlid mandible: the molecular basis of alternate feeding strategies. *Proc. Natl. Acad. Sci. USA* **102**, 16287-16292.
Alexander, C., Zuniga, E., Blitz, I. L., Wada, N., Le Pabic, P., Javidan, Y., Zhang, T., Cho, K. W., Gage Crump, J. and Schilling, T. F. (2011). Combinatorial roles for BMPs and Endothelin 1 in patterning the dorsal-ventral axis of the craniofacial skeleton. *Development* **138**, 5135-5146.
Barbosa, A. C., Funato, N., Chapman, S., McKee, M. D., Richardson, J. A., Olson, E. N. and Yanagisawa, H. (2007). Hand transcription factors cooperatively regulate development of the distal midline mesenchyme. *Dev. Biol.* **310**, 154-168.
Bartel, D. P. (2009). MicroRNAs: target recognition and regulatory functions. *Cell* **136**, 215-233.
Belteki, G., Haigh, J., Kabacs, N., Haigh, K., Sison, K., Costantini, F., Whitsett, J., Quaggin, S. E. and Nagy, A. (2005). Conditional and inducible transgene expression in mice through the combinatorial use of Cre-mediated recombination and tetracycline induction. *Nucleic Acids Res.* **33**, e51.
Britanova, O., Depew, M. J., Schwark, M., Thomas, B. L., Miletich, I., Sharpe, P. and Tarabykin, V. (2006). Satb2 haploinsufficiency phenocopies 2q32-q33 deletions, whereas loss suggests a fundamental role in the coordination of jaw development. *Am. J. Hum. Genet.* **79**, 668-678.
Brunet, L. J., McMahon, J. A., McMahon, A. P. and Harland, R. M. (1998). Noggin, cartilage morphogenesis, and joint formation in the mammalian skeleton. *Science* **280**, 1455-1457.
Chai, Y. and Maxson, R. E., Jr (2006). Recent advances in craniofacial morphogenesis. *Dev. Dyn.* **235**, 2353-2375.
Chai, Y., Jiang, X., Ito, Y., Bringas, P., Jr, Han, J., Rowitch, D. H., Soriano, P., McMahon, A. P. and Sucov, H. M. (2000). Fate of the mammalian cranial neural crest during tooth and mandibular morphogenesis. *Development* **127**, 1671-1679.
Charite, J., McFadden, D. G., Merlo, G., Levi, G., Clouthier, D. E., Yanagisawa, M., Richardson, J. A. and Olson, E. N. (2001). Role of Dlx6 in regulation of an endothelin-1-dependent, dHAND branchial arch enhancer. *Genes Dev.* **15**, 3039-3049.
Chen, R. M., Lin, Y. L. and Chou, C. W. (2010). GATA-3 transduces survival signals in osteoblasts through upregulation of bcl-x(L) gene expression. *J. Bone Miner. Res.* **25**, 2193-2204.
Chen, X., Xu, H., Yuan, P., Fang, F., Huss, M., Vega, V. B., Wong, E., Orlov, Y. L., Zhang, W., Jiang, J. et al. (2008). Integration of external signaling pathways with the core transcriptional network in embryonic stem cells. *Cell* **133**, 1106-1117.
Choi, M., Stottmann, R. W., Yang, Y. P., Meyers, E. N. and Klingensmith, J. (2007). The bone morphogenetic protein antagonist noggin regulates mammalian cardiac morphogenesis. *Circ. Res.* **100**, 220-228.
Danielian, P. S., Muccino, D., Rowitch, D. H., Michael, S. K. and McMahon, A. P. (1998). Modification of gene activity in mouse embryos in utero by a tamoxifen-inducible form of Cre recombinase. *Curr. Biol.* **8**, 1323-1326.
Davis, B. N., Hilyard, A. C., Lagna, G. and Hata, A. (2008). SMAD proteins control DROSHA-mediated microRNA maturation. *Nature* **454**, 56-61.
Depew, M. J., Lufkin, T. and Rubenstein, J. L. (2002). Specification of jaw subdivisions by Dlx genes. *Science* **298**, 381-385.
Dobreva, G., Chahrour, M., Dautzenberg, M., Chirivella, L., Kanzler, B., Farinas, I., Karsenty, G. and Grosschedl, R. (2006). SATB2 is a multifunctional determinant of craniofacial patterning and osteoblast differentiation. *Cell* **125**, 971-986.
Fei, T., Xia, K., Li, Z., Zhou, B., Zhu, S., Chen, H., Zhang, J., Chen, Z., Xiao, H., Han, J. D. et al. (2010). Genome-wide mapping of SMAD target genes reveals the role of BMP signaling in embryonic stem cell fate determination. *Genome Res.* **20**, 36-44.
Fragiadaki, M., Ikeda, T., Witherden, A., Mason, R. M., Abraham, D. and Bou-Gharios, G. (2011). High doses of TGF-beta potently suppress type I collagen via the transcription factor CUX1. *Mol. Biol. Cell* **22**, 1836-1844.
Funato, N., Chapman, S. L., McKee, M. D., Funato, H., Morris, J. A., Shelton, J. M., Richardson, J. A. and Yanagisawa, H. (2009). Hand2 controls osteoblast differentiation in the branchial arch by inhibiting DNA binding of Runx2. *Development* **136**, 615-625.
Gitton, Y., Heude, E., Vieux-Rochas, M., Benouaiche, L., Fontaine, A., Sato, T., Kurihara, Y., Kurihara, H., Couly, G. and Levi, G. (2010). Evolving maps in craniofacial development. *Semin. Cell Dev. Biol.* **21**, 301-308.
Gong, Y., Krakow, D., Marcelino, J., Wilkin, D., Chitayat, D., Babul-Hirji, R., Hudgins, L., Cremers, C. W., Cremers, F. P., Brunner, H. G. et al. (1999). Heterozygous mutations in the gene encoding noggin affect human joint morphogenesis. *Nat. Genet.* **21**, 302-304.
He, F., Xiong, W., Wang, Y., Matsui, M., Yu, X., Chai, Y., Klingensmith, J. and Chen, Y. (2010). Modulation of BMP signaling by Noggin is required for the maintenance of palatal epithelial integrity during palatogenesis. *Dev. Biol.* **347**, 109-121.
Ishii, M., Merrill, A. E., Chan, Y. S., Gitelman, I., Rice, D. P., Sucov, H. M. and Maxson, R. E., Jr (2003). Msx2 and Twist cooperatively control the development of the neural crest-derived skeletogenic mesenchyme of the murine skull vault. *Development* **130**, 6131-6142.
Ishii, M., Han, J., Yen, H. Y., Sucov, H. M., Chai, Y. and Maxson, R. E., Jr (2005). Combined deficiencies of Msx1 and Msx2 cause impaired patterning and survival of the cranial neural crest. *Development* **132**, 4937-4950.
Iulianella, A., Sharma, M., Durnin, M., Vanden Heuvel, G. B. and Trainor, P. A. (2008). Cux2 (Cutl2) integrates neural progenitor development with cell-cycle progression during spinal cord neurogenesis. *Development* **135**, 729-741.
Iulianella, A., Sharma, M., Vanden Heuvel, G. B. and Trainor, P. A. (2009). Cux2 functions downstream of Notch signaling to regulate dorsal interneuron formation in the spinal cord. *Development* **136**, 2329-2334.
Kirilly, D., Spana, E. P., Perrimon, N., Padgett, R. W. and Xie, T. (2005). BMP signaling is required for controlling somatic stem cell self-renewal in the Drosophila ovary. *Dev. Cell* **9**, 651-662.
Liu, W., Selever, J., Wang, D., Lu, M. F., Moses, K. A., Schwartz, R. J. and Martin, J. F. (2004). Bmp4 signaling is required for outflow-tract septation and branchial-arch artery remodeling. *Proc. Natl. Acad. Sci. USA* **101**, 4489-4494.
Liu, W., Selever, J., Murali, D., Sun, X., Brugger, S. M., Ma, L., Schwartz, R. J., Maxson, R., Furuta, Y. and Martin, J. F. (2005a). Threshold-specific requirements for Bmp4 in mandibular development. *Dev. Biol.* **283**, 282-293.
Liu, W., Sun, X., Braut, A., Mishina, Y., Behringer, R. R., Mina, M. and Martin, J. F. (2005b). Distinct functions for Bmp signaling in lip and palate fusion in mice. *Development* **132**, 1453-1461.
Luna-Zurita, L., Prados, B., Grego-Bessa, J., Luxan, G., del Monte, G., Benguria, A., Adams, R. H., Perez-Pomares, J. M. and de la Pompa, J. L. (2010). Integration of a Notch-dependent mesenchymal gene program and Bmp2-driven cell invasiveness regulates murine cardiac valve formation. *J. Clin. Invest.* **120**, 3493-3507.
Ma, L. and Martin, J. F. (2005). Generation of a Bmp2 conditional null allele. *Genesis* **42**, 203-206.
Ma, L., Lu, M. F., Schwartz, R. J. and Martin, J. F. (2005). Bmp2 is essential for cardiac cushion epithelial-mesenchymal transition and myocardial patterning. *Development* **132**, 5601-5611.
McFadden, D. G., Barbosa, A. C., Richardson, J. A., Schneider, M. D., Srivastava, D. and Olson, E. N. (2005). The Hand1 and Hand2 transcription factors regulate expansion of the embryonic cardiac ventricles in a gene dosage-dependent manner. *Development* **132**, 189-201.
Merrill, A. E., Eames, B. F., Weston, S. J., Heath, T. and Schneider, R. A. (2008). Mesenchyme-dependent BMP signaling directs the timing of mandibular osteogenesis. *Development* **135**, 1223-1234.
Mitsiadis, T. A., Angeli, I., James, C., Lendahl, U. and Sharpe, P. T. (2003). Role of Islet1 in the patterning of murine dentition. *Development* **130**, 4451-4460.
Paulsen, M., Legewie, S., Eils, R., Karaulanov, E. and Niehrs, C. (2011). Negative feedback in the bone morphogenetic protein 4 (BMP4) synexpression group governs its dynamic signaling range and canalizes development. *Proc. Natl. Acad. Sci. USA* **108**, 10202-10207.
Prall, O. W., Menon, M. K., Solloway, M. J., Watanabe, Y., Zaffran, S., Bajolle, F., Biben, C., McBride, J. J., Robertson, B. R., Chaulet, H. et al. (2007). An Nkx2-5/Bmp2/Smad1 negative feedback loop controls heart progenitor specification and proliferation. *Cell* **128**, 947-959.
Ralston, A., Cox, B. J., Nishioka, N., Sasaki, H., Chea, E., Rugg-Gunn, P., Guo, G., Robson, P., Draper, J. S. and Rossant, J. (2010). Gata3 regulates trophoblast development downstream of Tead4 and in parallel to Cdx2. *Development* **137**, 395-403.
Ruest, L.-B., Xiang, X., Lim, K.-C., Levi, G. and Clouthier, D. E. (2004). Endothelin A receptor-dependent and independent signaling pathways in establishing mandibular identity. *Development* **131**, 4413-4423.
Shen, T., Aneas, I., Sakabe, N., Dirschinger, R. J., Wang, G., Smemo, S., Westlund, J. M., Cheng, H., Dalton, N., Gu, Y. et al. (2011). Tbx20 regulates a genetic program essential to adult mouse cardiomyocyte function. *J. Clin. Invest.* **121**, 4640-4654.
Sheng, N., Xie, Z., Wang, C., Bai, G., Zhang, K., Zhu, Q., Song, J., Guillemot, F., Chen, Y. G., Lin, A. et al. (2010). Retinoic acid regulates bone morphogenic

protein signal duration by promoting the degradation of phosphorylated Smad1. *Proc. Natl. Acad. Sci. USA* **107**, 18886-18891.

Suzuki, S., Marazita, M. L., Cooper, M. E., Miwa, N., Hing, A., Jugessur, A., Natsume, N., Shimozato, K., Ohbayashi, N., Suzuki, Y. et al. (2009). Mutations in BMP4 are associated with subepithelial, microform, and overt cleft lip. *Am. J. Hum. Genet.* **84**, 406-411.

Tsarovina, K., Reiff, T., Stubbusch, J., Kurek, D., Grosveld, F. G., Parlato, R., Schutz, G. and Rohrer, H. (2010). The Gata3 transcription factor is required for the survival of embryonic and adult sympathetic neurons. *J. Neurosci.* **30**, 10833-10843.

Wang, J., Greene, S. B., Bonilla-Claudio, M., Tao, Y., Zhang, J., Bai, Y., Huang, Z., Black, B. L., Wang, F. and Martin, J. F. (2010). Bmp signaling regulates myocardial differentiation from cardiac progenitors through a MicroRNA-mediated mechanism. *Dev. Cell* **19**, 903-912.

Wang, J., Greene, S. B. and Martin, J. F. (2011). BMP signaling in congenital heart disease: new developments and future directions. *Birth Defects Res. A Clin. Mol. Teratol.* **91**, 441-448.

Wu, P., Jiang, T. X., Suksaweang, S., Widelitz, R. B. and Chuong, C. M. (2004). Molecular shaping of the beak. *Science* **305**, 1465-1466.

Xu, X., Han, J., Ito, Y., Bringas, P., Jr, Deng, C. and Chai, Y. (2008). Ectodermal Smad4 and p38 MAPK are functionally redundant in mediating TGF-beta/BMP signaling during tooth and palate development. *Dev. Cell* **15**, 322-329.

Ying, Q. L., Nichols, J., Chambers, I. and Smith, A. (2003). BMP induction of Id proteins suppresses differentiation and sustains embryonic stem cell self-renewal in collaboration with STAT3. *Cell* **115**, 281-292.

Zuniga, E., Rippen, M., Alexander, C., Schilling, T. F. and Crump, J. G. (2011). Gremlin 2 regulates distinct roles of BMP and Endothelin 1 signaling in dorsoventral patterning of the facial skeleton. *Development* **138**, 5147-5156.